Appendix A
Complete Transport Results of QAHE

Besides the transport results in Chap. 5, here we will show the complete data of quantum anomalous Hall effect (the same sample in Fig. 5.5). Figure A.1a, b displays the magnetic hysteresis loops of ρ_{yx} at different bottom-gate voltages (V_gs). At zero field, $\rho_{yx}(0)$ increases from 0.5 (h/e^2) at $V_g = -55$ V to 1 (h/e^2) at $V_g = -1.5$ V and then decreases to 0.59 (h/e^2) at $V_g = 200$ V. Figure A.1c, d displays the MR curves at different V_gs, which show a more complex behavior.

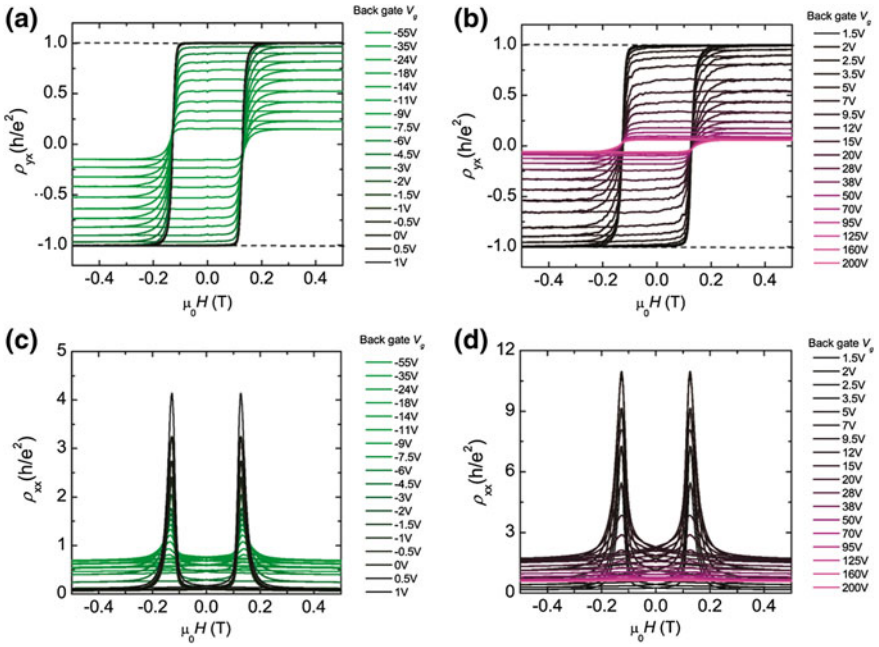

Fig. A.1 The complete transport data on the 5 QL $Cr_{0.15}(Bi_{0.1}Sb_{0.9})_{1.85}Te_3$ film on $SrTiO_3$ (111) substrate. **a** Hysteresis loops of ρ_{yx} with V_g varying from −55 to 1 V. **b** Hysteresis loops of ρ_{yx} with V_g varying from 1.5 to 200 V. **c** MR curves with V_g varying from −55 to 1 V. **d** MR curves with V_g varying from 1.5 to 200 V

J. Zhang, *Transport Studies of the Electrical, Magnetic and Thermoelectric Properties of Topological Insulator Thin Films*, Springer Theses,
DOI 10.1007/978-3-662-49927-6

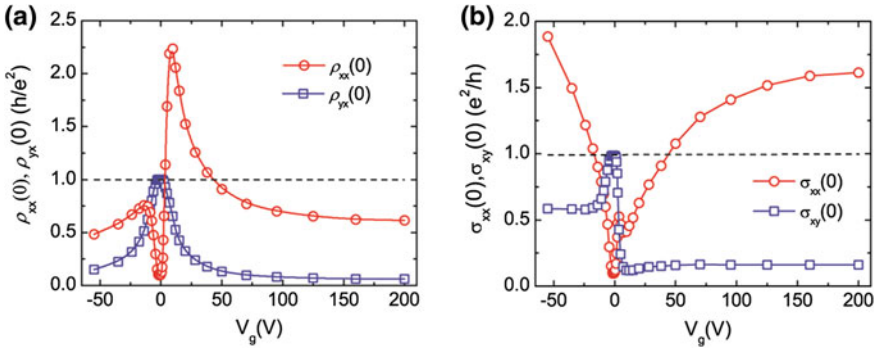

Fig. A.2 The large-scale results of $\rho_{yx}(0)$, $\rho_{xx}(0)$ (**a**), and $\sigma_{xy}(0)$, $\sigma_{xx}(0)$ (**b**) on the dependence of V_g

Figure A.2a presents V_g-dependent $\rho_{yx}(0)$ and $\rho_{xx}(0)$ with V_g varying from −55 to 200 V. $\rho_{yx}(0)$ shows a plateau around $V_g = -1.5$ V. $\rho_{xx}(0)$ exhibits a double-peak structure, with a dip between two peaks also located at $V_g = -1.5$ V. Outside the two $\rho_{xx}(0)$ peaks, $\rho_{yx}(0)$ and $\rho_{xx}(0)$ basically have similar V_g dependence, which is due to V_g-induced variation in carrier density. Figure A.2b shows the corresponding zero field σ_{xy} and σ_{xx} (indicated by $\sigma_{xy}(0)$ and $\sigma_{xx}(0)$, respectively). The curves exhibit similar V_g dependence with $\rho_{yx}(0)$ and $\rho_{xx}(0)$ near $V_g = -1.5$ V.

Appendix B
Simple Picture for the Sign of AHE

In Chap. 4 of the main text, we have presented a magnetic quantum phase transition accompanied by the sign reversal of the anomalous Hall effect (AHE) across the quantum critical point (QCP) in 8 QL Cr-doped $Bi_2(Se_xTe_{1-x})_3$ films at the base temperature. Here, we report a simple picture to understand the sign change of AHE conductance σ_{xy} in the *n*-doped regime.

In order to take into account the quantum confinement along z direction, an approximation is applied for the *n*th bulk sub-bands by treating $\langle k_z^2 \rangle = (n\pi/d)^2$ and $\langle k_z \rangle = 0$ (Ref. [1] in the main text). The couplings between sub-bands with different *n* are neglected in this approximation. We emphasize that this approximation can be used for bulk sub-band since the coupling between different sub-bands is weak once they are well-separated in energy, but it will miss surface states because the surface states originate from the linear k term in the off-diagonal part of Hamiltonian [Eq. (4.2) in Chap. 4], which is neglected. However, in the metallic regime, the main physics should be dominated by the bulk carriers so that it is useful to apply this approximation to understanding the underlying physics. Then in the basis as $|+,\uparrow\rangle$, $|-,\downarrow\rangle$, $|+,\downarrow\rangle$ and $|-,\uparrow\rangle$, the Hamiltonian for the *n*th sub-bands is simplified as follows:

$$H_0(n) = \tilde{\epsilon}_{k_\parallel} + \begin{pmatrix} \widetilde{M}(k_\parallel) & A_0(k_y + ik_x) & 0 & 0 \\ A_0(k_y - ik_x) & -\widetilde{M}(k_\parallel) & 0 & 0 \\ 0 & 0 & \widetilde{M}(k_\parallel) & A_0(k_y - ik_x) \\ 0 & 0 & A_0(k_y + ik_x) & -\widetilde{M}(k_\parallel) \end{pmatrix}, \tag{B.1}$$

where $\tilde{\epsilon}_{k_\parallel} = C_0 + C_1(n\pi/d)^2 + C_2 k_\parallel^2 = \widetilde{C}_0 + C_2 k_\parallel^2$, $\widetilde{M}(k_\parallel) = M_0 + M_1(n\pi/d)^2 + M_2 k_\parallel^2 = \widetilde{M}_0 + M_2 k_\parallel^2$, and

J. Zhang, *Transport Studies of the Electrical, Magnetic and Thermoelectric Properties of Topological Insulator Thin Films*, Springer Theses,
DOI 10.1007/978-3-662-49927-6

$$H_Z = \begin{pmatrix} G_{z1}+G_{z2} & & & \\ & -G_{z1}+G_{z2} & & \\ & & -G_{z1}-G_{z2} & \\ & & & G_{z1}-G_{z2} \end{pmatrix} \tag{B.2}$$

Now it is clear that the approximated Hamiltonian is block diagonal with each block taking the form of 2D Dirac Hamiltonian, and correspondingly the four bands can be divided into two groups, one mainly consists of $|+,\uparrow\rangle$ and $|-,\downarrow\rangle$ components, forming the bands $|C_1\rangle$ and $|V_1\rangle$ as shown by the red line in Fig. B.1a, b, while the other one consists of $|+,\downarrow\rangle$ and $|-,\uparrow\rangle$ components, forming the bands $|C_2\rangle$ and $|V_2\rangle$, as shown by the blue line in Fig. B.1a, b. The band $|C_1(V_1)\rangle$ is related to $|C_2(V_2)\rangle$ by TR operation. With zero magnetization, σ_{xy} from these two groups always takes the opposite sign and cancels each other, no matter in the inverted or normal regime. However, the σ_{xy} for each 2×2 block of the Hamiltonian behaves quite different for the normal and inverted regime. For the normal regime, σ_{xy} from one single group will drop to zero when μ is in the gap, while it stays at some finite maximum values for the inverted regime, as shown in Fig. B.1c, d.

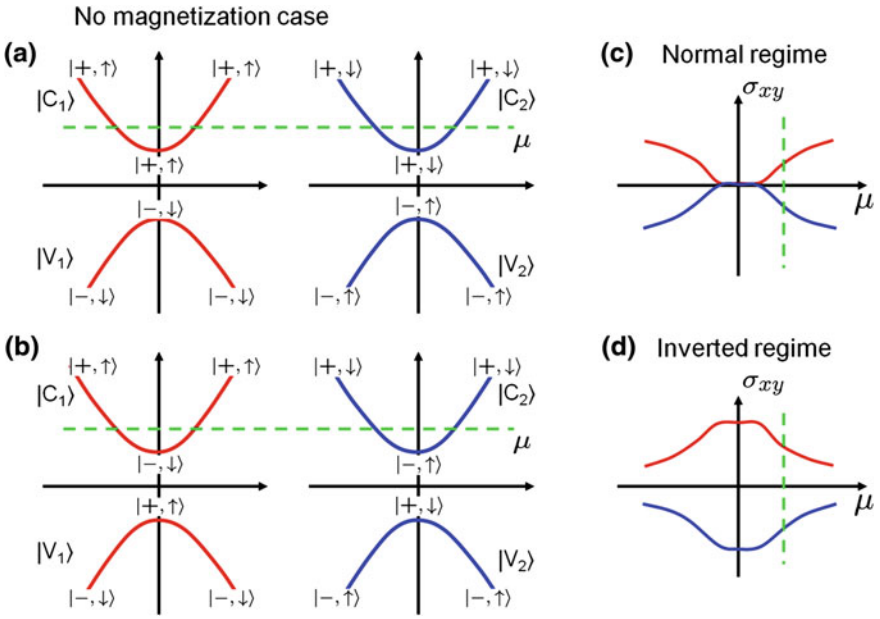

Fig. B.1 The schematic of bulk sub-band dispersion is shown in **a** for the normal regime and **b** for the inverted case. **c**, **d** The σ_{xy} of each group for the normal and inverted regimes. Here, both G_{z1} and G_{z2} are zero

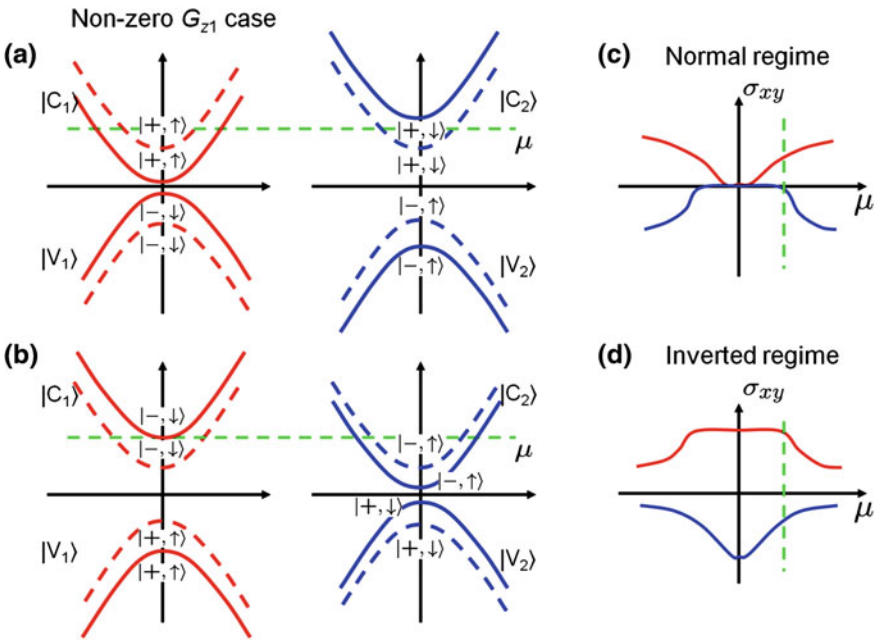

Fig. B.2 The schematic of bulk sub-band dispersion is shown in **a** for the normal regime and **b** for the inverted case. **c**, **d** The σ_{xy} of each group for the normal and inverted regimes. Here, G_{z1} is nonzero, G_{z2} is zero

When the ferromagnetism is introduced, the G_{z1} and G_{z2} terms should be treated separately. For G_{z1} term, it takes the opposite sign for the two states within one block in the Hamiltonian and increases the band gap for one block but decreases the band gap for the other one, as shown in Fig. B.2a, b. Consequently, it will induce different μ dependence of σ_{xy} of the two blocks. However, we can see from Fig. B.2c, d that once G_{z1} is fixed, the total σ_{xy} always takes the same sign, no matter in the normal or inverted regime. For G_{z2} term, it has the same sign within one block and opposite sign for different blocks. Therefore, it shifts the bands in one block up and the other block down (Fig. B.3a, b). Such a shift leads to the differences between the inverted and normal regimes, and hence, the sign change of

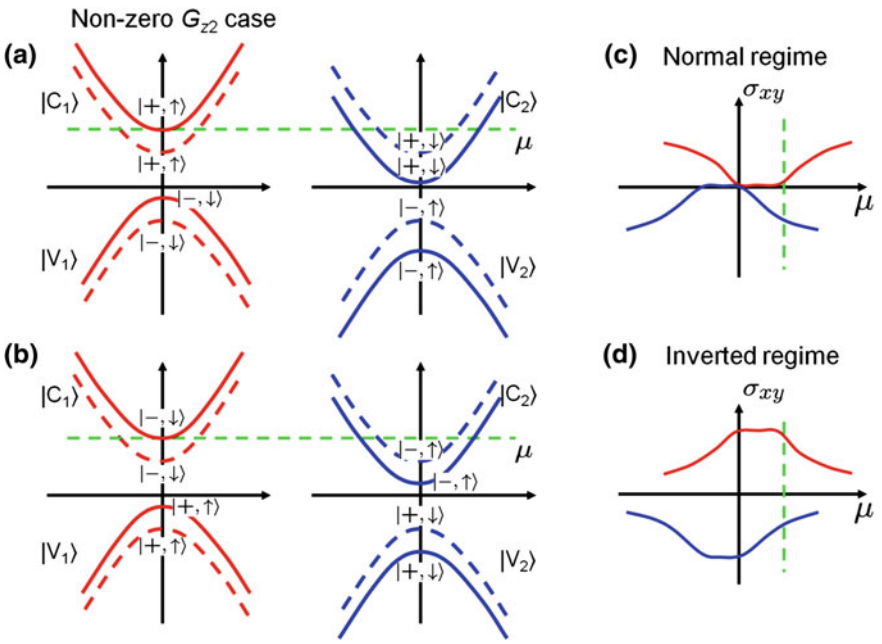

Fig. B.3 The schematic of bulk sub-band dispersion is shown in **a** for the normal regime and **b** for the inverted case. **c**, **d** The σ_{xy} of each group for the normal and inverted regimes. Here, G_{z1} is zero, G_{z2} is nonzero

the total σ_{xy} is shown in Fig. B.3c, d. Therefore, our simple picture here explains the numerical results for σ_{xy}. Compared with the experiment, our numerical results indicate that the influence of the magnetization should be dominated by the G_{z2} term. However, we do not know how the other mechanism, such as skew scattering or side jump, contributes to σ_{xy}, and therefore, we cannot exclude other possibilities.

Reference

1. Liu C-X, Zhang H, Yan B, et al. Oscillatory crossover from two-dimensional to three-dimensional topological insulators. Phys Rev B. 2010;81:041307.